traces are reduced to obtain the actual core diameter at any test temperature. Equation (4) is employed to calculate maximum tangential strain.

Conclusions

Laboratory uniaxial tensile data, while valuable for comparative purposes in propellant development programs, generally do not provide the stress engineer with sufficient information upon which to base predictions of solid rocket motor performance. Rate effects, often neglected in testing for screening purposes, can introduce wide discrepancies between propellant strain capabilities as measured in constant-strain rate tests and the performance of propellant in a motor during low-temperature storage. Even strain endurance capability of propellant appears to be a time-dependent property, since it varies with the rate at which the constant strain was originally imposed on the propellant. Finally, test techniques have not been developed as yet to the point where adequate failure criteria for propellants in combined stress or strain states have been defined.

Model test motors are, therefore, of considerable usefulness in aiding the prediction of structural performance of solid rocket motors. A simple, cylindrical motor 2 in. in diameter and 12 in. long has been used successfully to define the threshold of propellant failure in terms of strain induced by low-temperature conditioning. Proper selection of the internal perforation in the test motor allows a comparison of strains experienced in the test motor with those experienced in prototype cylindrical core rocket motors. When the size of the internal perforations in such motors is small ($\doteq$ 0.25 in.), strain relief due to "end effects" is apparent over the entire length of the motor. A finite difference solution is appropriate in such cases.[2] An example of the results that can be obtained by this technique is shown in Fig. 9. To achieve a plane strain condition, the length of the motor should be increased. When larger internal perforations are employed, a finite-length section of uniform maximum strain is observed at the axial center of the motor, suggesting that the propellant in this region approaches a state of plane strain.

References

[1] Wiegand, J. H., "Study of mechanical properties of solid rocket propellants," Aerojet-General Corp. Rept. 0411-10F (March 1962).

[2] Ignatowski, A. J. and Jenkins, L. W., "Polymer physics," Rohm & Haas Co., Progr. Rept. on Interior Ballistics, P-62-1 (August 1962).

[3] Parr, C. H., "End effects due to shrinkage in solid propellent grains," Bull. Twentieth Meeting, JANAF-ARPA-NASA Panel on Physical Properties, Vol. I, SPIA/PP14U, p. 71 (October 1961).

[4] Williams, M. L., Blatz, P. J., and Shapery, R. A., "Fundamental studies relating to systems analysis of solid propellants," Graduate Aeronaut. Lab., Calif. Inst. Tech. SM61-5 (February 1961).

[5] Fourney, M. E. and Parmerter, R. R., "Stress-concentration data for internally perforated star grains," Naval Ordnance Test Station TP 2728, Bur. Naval Weapons 7758 (December 1961).

[6] Williams, M. L., "Some thermal stress design data for rocket grains," ARS J. 29, 260–267 (1959).

[7] Medford, J. E., "Measurement of thermal diffusivity of solid propellants," ARS J. 32, 1390–1392 (1962).

[8] Wiegand, J. H., "Recent advances in mechanical properties evaluation of solid propellants," ARS J. 32, 521–527 (1962).

OCTOBER 1963 AIAA JOURNAL VOL. 1, NO. 10

Nonuniform Shrinkage of a Hollow Viscoelastic Cylinder

A. S. Cakmak*
Princeton University, Princeton, N. J.

The effects of nonuniform shrinkage on stresses and displacements of a thick-walled, hollow cylinder of viscoelastic material are discussed, for the case of plane strain, as a function of the loading rate. The cylinder is contained in a rigid casing resulting in zero circumferential and radial displacements at the outer surface. The inner surface is free of tractions. The problem is solved using the elastic-viscoelastic analogy, where the deviatoric behavior is characterized by the standard solid, and the volumetric behavior is taken to be elastic. The results indicate a strong dependence of radial displacements and principal stresses on the loading rate. The maximum values of the principal stresses show a marked reduction and smaller deviations from their final values for decreasing values of the loading rate. The radial displacements exhibit little change in deviation from their final values for changes of the loading rate.

Nomenclature

λ,μ = Lame's constants
r,z = cylindrical coordinates
u_r = radial displacement
σ_r = radial stress component
σ_θ = circumferential stress component
ϵ_r = radial strain component
ϵ_θ = circumferential strain component
S_{ij} = deviatoric stress components
e_{ij} = deviatoric strain components
θ = rate of loading parameter
E = Young's modulus
γ = Poisson's ratio
G = shear modulus
K = bulk modulus
μ_m = viscosity
δ_{ij} = Kronecker delta
$\mathbf{G}$ = viscoelastic shear modulus
$\mathbf{K}$ = viscoelastic bulk modulus
T = temperature
δT = difference in temperature
τ = relaxation time
$H(t)$ = Heaviside step function
C_1,C_2 = integration constants
a = inner radius
b = outer radius
L = Laplace transform
L^{-1} = inverse Laplace transform
S = Laplace transform parameter

Received March 4, 1963; revision received July 24, 1693. This research was supported by the Office of Naval Research under Contract Nonr 266(78) during the author's residence at Columbia University.

* Assistant Professor of Civil Engineering, Department of Civil Engineering, School of Engineering and Applied Science.

Introduction

IN the storage of solid fuel rockets, a certain radially dependent shrinkage of the fuel core may take place resulting in residual stresses in the structure. This paper analyzes the problem of a hollow viscoelastic cylinder encased within a rigid shell. The boundary conditions are such that the outer surface has no radial or circumferential displacements, whereas the inner surface is traction free (Fig. 1).

The effect of shrinkage is handled in the form of a temperature distribution problem, where multiplication by an appropriate coefficient of shrinkage results in the shrinkage distribution. Therefore, the problem is considered as a temperature distribution problem, where the space distribution of temperature (indirectly shrinkage) is arbitrary and the time distribution is exponential depending on a loading rate parameter θ.

Elastic Problem

The equilibrium equation for the thermoelastic problem, for plane strain and axial symmetry, in terms of displacements is[1]

$$\frac{d}{dr}\left[\frac{1}{r}\frac{d(ru_r)}{dr}\right] = \alpha_0(1+\gamma_0)\frac{dT(r)}{dr} \tag{1}$$

This is an ordinary differential equation with the solution

$$u_r(r) = \frac{(1+\gamma_0)}{r}\alpha_0\int_a^r T(r')r'dr' + C_1 r + \frac{C_2}{r} \tag{2}$$

where a is the inner radius, and

$$\alpha_0 = \alpha(1+\gamma) \qquad \gamma_0 = \frac{\gamma}{(1-\gamma)} \qquad E_0 = \frac{E}{1-\gamma^2}$$

From the strain-displacement relations

$$\epsilon_r = \partial u_r/\partial r \qquad \epsilon_\theta = u_r/r \tag{3}$$

and the stress-strain relations

$$\begin{aligned}\epsilon_r &= \frac{(1-\gamma^2)}{E}\left[\sigma_r - \frac{\gamma}{1-\gamma}\sigma_\theta\right]\\ \epsilon_\theta &= \frac{(1-\gamma^2)}{E}\left[\sigma_\theta - \frac{\gamma}{1-\gamma}\sigma_r\right]\end{aligned} \tag{4}$$

the principal stresses can be determined:

$$\begin{aligned}\sigma_r &= -\frac{\alpha_0 E_0}{r^2}\int_a^r T(r')r'dr' + \frac{C_1E_0}{1-\gamma_0} - \frac{E_0C_2}{(1+\gamma_0)}r^2\\ \sigma_\theta &= \frac{\alpha_0E_0}{r^2}\int_a^r T(r')r'dr' - \alpha_0E_0T(r) + \frac{E_0C_1}{1-\gamma_0} + \frac{E_0C_2}{(1+\gamma)}r^2\end{aligned} \tag{5}$$

To evaluate the constants C_1, C_2, use the following boundary conditions:

$$\sigma_r]_{r=a} = 0 \qquad u_r]_{r=b} = 0 \tag{6}$$

where b is the outer radius and a the inner radius. Therefore, one gets

$$\begin{aligned}C_1 &= -\frac{(1-\gamma_0)(1+\gamma_0)\alpha_0}{b^2(1-\gamma_0)+a^2(1+\gamma_0)}\int_a^b T(r)rdr\\ C_2 &= -\frac{(1+\gamma_0)^2a^2\alpha_0}{b^2(1-\gamma_0)+a^2(1+\gamma_0)}\int_a^b T(r)rdr\end{aligned} \tag{7}$$

Replacing the elastic constants E,γ by G,K

$$E = \frac{9GK}{3K+G} \qquad \gamma = \frac{3K-2G}{6K+2G}$$

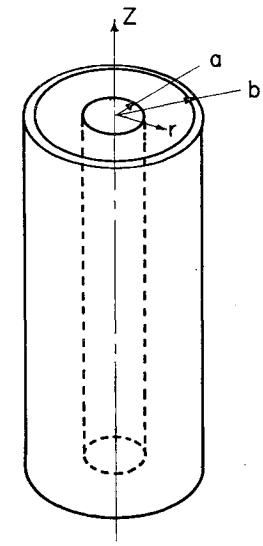

Fig. 1 The hollow cylinder.

yields the elastic solution:

$$\left.\begin{aligned}\sigma_r(r) &= -\frac{18GK\alpha}{4G+3K}\left[\frac{1}{r^2}\int_a^r T(r')r'dr' + \frac{G+3K(1-a^2/r^2)}{G(a^2+3b^2)+3Ka^2}\int_a^b T(r)rdr\right]\\ \sigma_\theta(r) &= -\frac{18\,GK\alpha}{4G+3K}\left[T(r) - \frac{1}{r^2}\int_a^r T(r')r'dr' + \frac{G+3K(1+a^2/r^2)}{G(a^2+3b^2)+3Ka^2}\int_a^b T(r)rdr\right]\\ u_r(r) &= -\frac{9K\alpha}{4G+3K}\left[\frac{1}{r}\int_a^r T(r')r'dr' - \frac{3Gr+(3K+G)a^2/r^2}{3Gb^2+(3K+G)a^2}\int_a^b T(r)rdr\right]\end{aligned}\right\} \tag{8}$$

Models of Viscoelastic Response

As mentioned before, the volumetric behavior is elastic, and the deviatoric behavior is that of a standard solid, Fig. 2:

$$\begin{aligned}\sigma_{kk} &= 3\mathbf{K}\epsilon_{kk}\\ S_{ij} + \tau\dot{S}_{ij} &= 2Ge_{ij} + 2G\,\tau_u\dot{e}_{ij}\end{aligned} \tag{9}$$

where

$$\cdot = d/dt \qquad \tau = \mu_m/G_m \qquad \tau_u = \tau[1+(G_m/G)]$$

$$\epsilon_{ij} = e_{ij} + \tfrac{1}{3}\delta_{ij}\epsilon_{kk} \qquad \sigma_{ij} = S_{ij} + \tfrac{1}{3}\delta_{ij}\sigma_{kk}$$

Application of the Laplace transform[2]

$$\mathcal{L}\{f(t)\} = \int_0^\infty f(t)e^{-st}\,dt = f(s) \tag{10}$$

to Eq. (9) results in

$$\bar{\sigma}_{kk}(s) = 3\bar{\mathbf{K}}(s)\bar{\epsilon}_{kk}(s) \qquad \bar{S}_{ij}(s) = 2\bar{\mathbf{G}}(s)\dot{e}_{ij}(s) \tag{11}$$

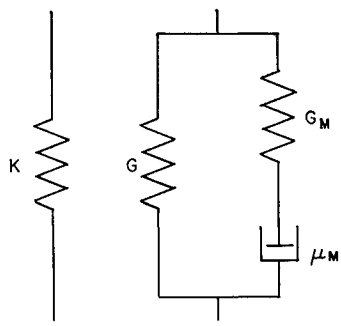

Fig. 2 The models of mechanical response of the material; a) volumetric, b) deviatoric.

where

$$\bar{K}(s) = K \qquad \bar{G}(s) = G\frac{(1 + s\tau_u)}{(1\ s\tau)}$$

Application of the Elastic-Viscoelastic Analogy

Let the shrinkage distribution be given by

$$\alpha T(t,r) = \alpha\delta T\ T_0(r)\ H(t)(1 - e^{-t/\theta}) \tag{12}$$

where $H(t)$ is the Heaviside step function, $\alpha\delta T$ the difference in shrinkage between the inside and outside of the cylinder, and θ is the loading rate parameter determining the rate of shrinkage (e.g., for $\theta = 0$, one has a step loading; for $\theta > 0$, one has an exponential loading).

Application of the Laplace transform to the elastic solution[3] and the replacement of the transformed elastic constants by their transformed operational counterparts yields

$$\left.\begin{aligned}
\bar{u}_r(r,s) &= D_1(1 + S\tau)\left[-\frac{1}{(S + 1/\theta)(S + B/\tau_B)} + \frac{1}{S(S + B/\tau_B)}\right] + D_2[A + (A\tau + \tau_A)S + \tau\tau_A S^2]\cdot \\
&\quad \left[-\frac{1}{(S + 1/\theta)(S + B/\tau_B)(S + C/\tau_C)} + \frac{1}{S(S + B/\tau_B)(S + C/\tau_C)}\right] \\
-\bar{\sigma}_r(r,s) &= \\
&\quad D_3(1 + S\tau_u)\left[-\frac{1}{(S + 1/\theta)(S + B/\tau_B)} + \frac{1}{S(S + B/\tau_B)}\right] + D_4[A^* + (A^*\tau_u + \tau_A^*)S + \tau_u\tau_A^* S^2]\cdot \\
&\quad \left[-\frac{1}{(S + 1/\theta)(S + B/\tau_B)(S + C/\tau_C)} + \frac{1}{S(S + B/\tau_B)(S + C/\tau_C)}\right] \\
-\bar{\sigma}_\theta(r,s) &= [T_0(r) - D_3](1 + S\tau_u) - \left[\frac{1}{(S + 1/\theta)(S + B/\tau_B)} + \frac{1}{S(S + B/\tau_B)}\right] + \\
&\quad D_4^1[A^* + (A^*\tau_u + \tau_A^*)S + \tau_u\tau_A^* S^2]\cdot \\
&\quad \left[-\frac{1}{(S + 1/\theta)(S + B/\tau_B)(S + C/\tau_C)} + \frac{1}{S(S + B/\tau_B)(S + C/\tau_C)}\right]
\end{aligned}\right\} \tag{13}$$

where

$$\begin{aligned}
A &= 3Gr + 3Ka^2/r^2 + Ga^2/r^2 \\
\tau_A &= 3Gr\tau_u + 3K\tau a^2/r^2 + G\tau_u a^2/r^2 \\
B &= 3K + 4G \\
\tau_B &= 3K\tau + 4G\tau_u \\
C &= 3Gb^2 + 3Ka^2 + Ga^2 \\
\tau_C &= 3Gb^2\tau_u + 3Ka^2\tau + Ga^2\tau_u \\
A^* &= G + 3K \\
\tau_A^* &= G\tau_u + 3K\tau \\
D_1 &= \frac{9K\alpha}{r\tau_B}\int_a^b T_0^1(r')r'dr' \\
D_2 &= \frac{9K\alpha}{\tau_B\tau_C}\int_a^b T_0^1(r)dr \\
D_3 &= \frac{18\ KG\alpha}{r^2\tau_B}\int_a^r T_0^1(r')r'dr' \\
D_4 &= \frac{18\ KG\alpha(1 - a^2/r^2)}{\tau_B\tau_C}\int_a^b T_0^1(r)rdr \\
D_4^1 &= \frac{18\ KG\alpha(1 + a^2/r^2)}{\tau_B\tau_C}\int_a^b T_0^1(r)rdr \\
T_0^1(r) &= \delta T\ T_0(r)
\end{aligned}$$

To obtain the viscoelastic solution, the inverse Laplace transformation[2]

$$L^{-1}\{\bar{f}(S)\} = \frac{1}{2\pi i}\int_{\gamma - i\infty}^{\gamma + i\infty}\bar{f}(S)\ e^{st}\ ds = f(t) \tag{14}$$

is applied to Eq. (13), yielding the following relations for the radial displacement and the principal stresses:

$$\left.\begin{aligned}
\frac{u_r(r,t)}{u^1} &= \frac{I}{ar}\int_a^r T(r')r'dr' + \frac{\rho II}{[3\mu + \beta^2(\mu + 3\Gamma)]b^2}\int_a^b T_0^1(r)rdr \\
\frac{-\sigma_r(r,t)}{\sigma^1} &= \frac{I'}{r^2}\int_a^r T(r')r'dr' - \frac{(1 - 1/\rho^2)II'}{[3\mu + \beta^2(\mu + 3\Gamma)]b^2}\int_a^b T_0^1(r)rdr \\
\frac{-\sigma_\theta(r,t)}{\sigma^1} &= \left[T(r) - \frac{1}{r^2}\int_a^r T(r')r'dr'\right]I' - \frac{(1 + 1/\rho^2)II'}{[3\mu + \beta^2(\mu + 3\Gamma)]b^2}\int_a^b T_0^1(r)rdr
\end{aligned}\right\} \tag{15}$$

where

$$\begin{aligned}
\mu &= \tau_u/\tau \qquad \beta = a/b \\
\Gamma &= K/G \qquad u^1 = a\alpha\ \delta T[9\Gamma/(4\mu + 3\Gamma)] \\
\rho &= r/a \qquad \sigma^1 = \alpha\ \delta T[18\Gamma/(4\mu + 3\Gamma)]
\end{aligned}$$

and

$$\left.\begin{aligned}
I &= \frac{1}{\alpha_2} - \frac{(1 - \alpha_1)}{(\alpha_2 - \alpha_1)}e^{-\alpha_1 t/\tau} - (1 - \alpha_2)\left(\frac{1}{\alpha_1} - \frac{1}{\alpha_2 - \alpha_1}\right)e^{-\alpha_2 t/\tau} \\
II &= \frac{\alpha_3^1}{\alpha_2\alpha_3} + \frac{-\alpha_3^1 + (\alpha_3^1 + \bar{\alpha}_3^1)\alpha_1 - \bar{\alpha}_3^1\alpha_1^2}{(\alpha_2 - \alpha_1)(\alpha_1 - \alpha_3)}e^{-\alpha_1 t/\tau} - \left(\frac{1}{\alpha_2} - \frac{1}{\alpha_2 - \alpha_1}\right)\frac{-\alpha_3^1 + (\alpha_3^1 + \bar{\alpha}_3^1)\alpha_2 - \bar{\alpha}_3^1\alpha_2^2}{(\alpha_3 - \alpha_2)}\cdot \\
&\quad e^{-\alpha_2 t/\tau} + \left(\frac{1}{\alpha_3} - \frac{1}{\alpha_3 - \alpha_1}\right)\frac{-\alpha_3^1 + (\alpha_3^1 + \bar{\alpha}_3^1)\alpha_3 - \bar{\alpha}_3^1\alpha_3^2}{(\alpha_3 - \alpha_2)}e^{-\alpha_3 t/\tau} \\
I' &= \frac{1}{\alpha_2} - \frac{1 + \mu\alpha_1}{\alpha_2 - \alpha_1}e^{-\alpha_1 t/\tau} - (1 - \mu\alpha_2)\left(\frac{1}{\alpha_2} - \frac{1}{\alpha_2 - \alpha_1}\right)e^{-\alpha_2 t/\tau} \\
II' &= -\frac{\alpha_2^1}{\alpha_2\alpha_3} + \frac{\alpha_2^1 + (\alpha_2^1 + \bar{\alpha}_2^1)\alpha_1 - \mu\bar{\alpha}_2^1\alpha_1^2}{(\alpha_2 - \alpha_1)(\alpha_1 - \alpha_3)}e^{-\alpha_1 t/\tau} - \left(\frac{1}{\alpha_2} - \frac{1}{\alpha_2 - \alpha_3}\right)\cdot \\
&\quad \frac{-\alpha_2^1 + (\alpha_2^1 + \bar{\alpha}_2^1)\alpha_2 - \mu\bar{\alpha}_2^1\alpha_2^2}{(\alpha_3 - \alpha_2)}e^{-\alpha_2 t/\tau} + \left(\frac{1}{\alpha_3} - \frac{1}{\alpha_3 - \alpha_1}\right)\frac{-\alpha_2^1 + (\alpha_2^1 + \bar{\alpha}_2^1)\alpha_3 - \mu\bar{\alpha}_2^1\alpha_3^2}{(\alpha_3 - \alpha_2)}e^{-\alpha_3 t/\tau}
\end{aligned}\right\} \tag{16}$$

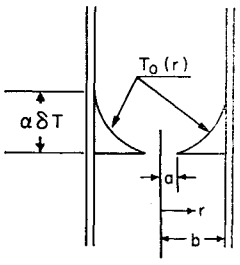

Fig. 3 The space distribution of shrinkage.

with

$$\alpha_1 = \frac{\tau}{\theta} \qquad \alpha_3 = \frac{3 + \beta^2(1 + 3\Gamma)}{3\mu + \beta^2(\mu + 3\Gamma)}$$

$$\alpha_2 = \frac{4 + 3\Gamma}{4\mu + 3\Gamma} \qquad \alpha_3{}^1 = 3 + \frac{1}{\rho^2}(1 + 3\Gamma)$$

$$\alpha_2{}^1 = 1 + 3\Gamma \qquad \bar{\alpha}_3{}^1 = 3\mu + \frac{1}{\rho^2}(\mu + 3\Gamma)$$

$$\bar{\alpha}_2{}^1 = \mu + 3\Gamma$$

Numerical Example

To illustrate the problem, a numerical example is considered. In this numerical example, the arbitrary space distribution of temperature is taken to be the steady-state solution of the heat conduction problem of the thick-walled cylinder subject to a fixed temperature difference between the inner and outer faces, as shown in Fig. 3:

$$T_0(r) = \frac{\log b/r}{\log a/b} \qquad T_0(\rho) = \frac{\log 1/\beta\rho}{\log 1/\beta} \tag{17}$$

The shrinkage is given by $\alpha\delta T T_0(r)$, where $\alpha\delta T$ is the difference in shrinkage between the inside surface and the outside surface of the cylinder. For this distribution, the integrals in Eqs. (15) yield

$$\int_a^r r' T_0(r')dr' = a^2 A(\rho) = \frac{a^2}{\log 1/\beta}\left(\frac{1}{2}\log\beta + \frac{\rho^2 - 1}{4} + \frac{\rho^2}{2}\log\frac{1}{\beta\rho}\right)$$

$$\int_a^b r' T_0(r')dr' = a^2 B(\beta) = \frac{a^2}{\log 1/\beta}\left(\frac{1}{2}\log\beta + \frac{1/\beta^2 - 1}{4}\right)$$

With these results, the viscoelastic solution becomes

$$\left.\begin{aligned} \frac{u_r(r,t)}{u^1} &= \frac{IA(\rho)}{\rho} + \frac{II\rho\beta\, A(\beta)}{3\mu + \beta^2(\mu + 3\Gamma)} \\ -\frac{\sigma_r(r,t)}{\sigma^1} &= \frac{I'A(\rho)}{\rho^2} - \frac{II'(1 - 1/\rho)\beta^2 A(\beta)}{3\mu + \beta^2(\mu + 3\Gamma)} \\ -\frac{\sigma_\theta(r,t)}{\sigma^1} &= I'\left[T_0(\rho) - \frac{A(\rho)}{\rho^2}\right] - \\ &\qquad II'\left(1 + \frac{1}{\beta}\right)\frac{\beta^2 A(\beta)}{3\mu + \beta^2(\mu + 3\Gamma)} \end{aligned}\right\} \tag{18}$$

In choosing numerical values for the elastic and viscoelastic constants, values corresponding to real materials will be picked; therefore, not assuming incompressibility, the following values are assumed:

$$\gamma = 0.3 \qquad G/G_m = 0.1 \qquad \beta = \tfrac{1}{3}$$

Since, in the elastic medium, Poisson's ratio γ is related to G and K by $G/K = 3(1 - 2\gamma)/2(1 + \gamma)$ and, in the standard solid, the forementioned G corresponds to the instantaneous response, one has $G_{\text{inst}} = G + G_M$.

Equations (18) are evaluated for this numerical example using four values of the loading rate parameter θ ranging from $\theta = 0$ (instantaneous loading) through the values $\theta = 0.25\tau$ and $\theta = 1.00\tau$ to $\theta = 4.00\tau$ (a rather slow loading). The results are exhibited graphically as follows:

1) The maximum values of stresses σ_r at $r = 2.50a$, σ_θ at $r = a$, and the radial displacement u_r at $r = a$ are plotted as dimensionless functions of time for the four values of the loading rate parameter, Fig. 4.

2) The values of σ_r, σ_θ, u_r, respectively, are plotted as dimensionless functions of the radius r for seven time inter-

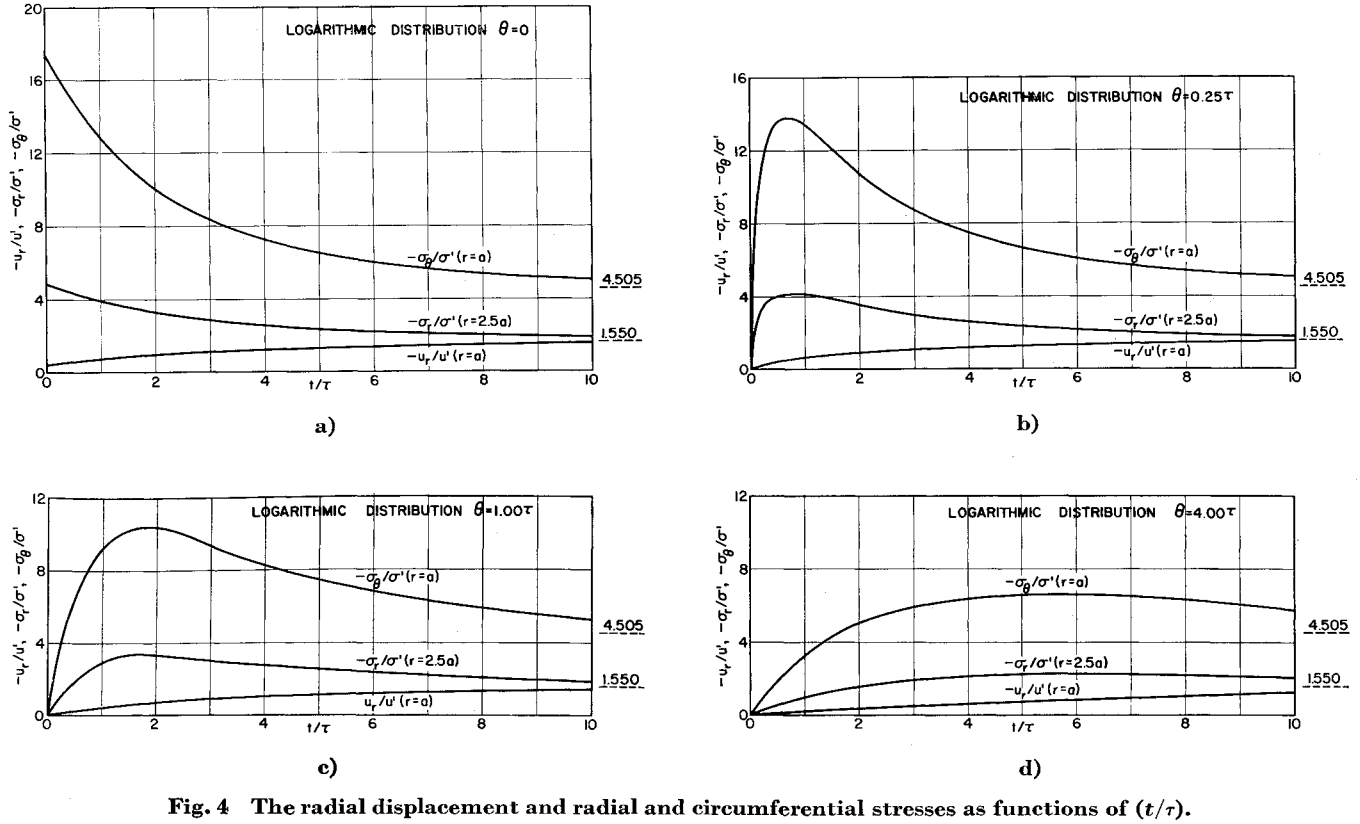

Fig. 4 The radial displacement and radial and circumferential stresses as functions of (t/τ).

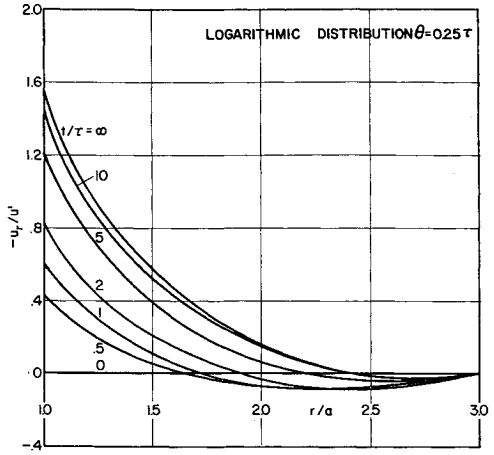

a)

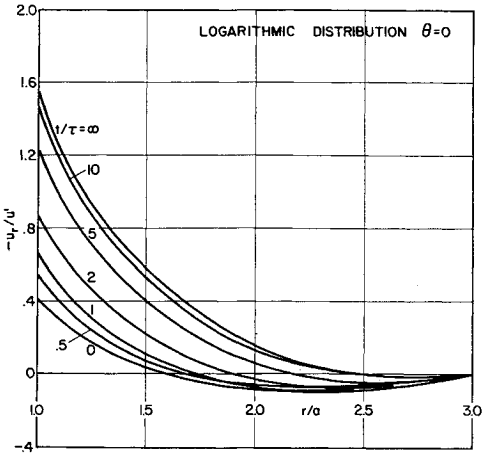

b)

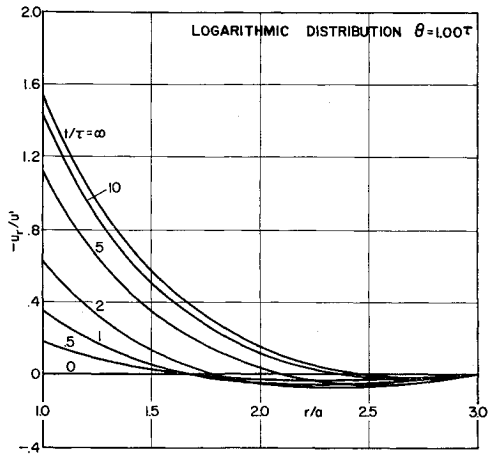

c)

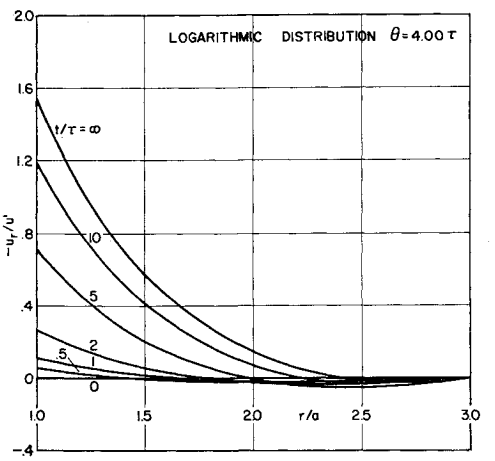

d)

Fig. 5 The radial displacement as a function of (r/a).

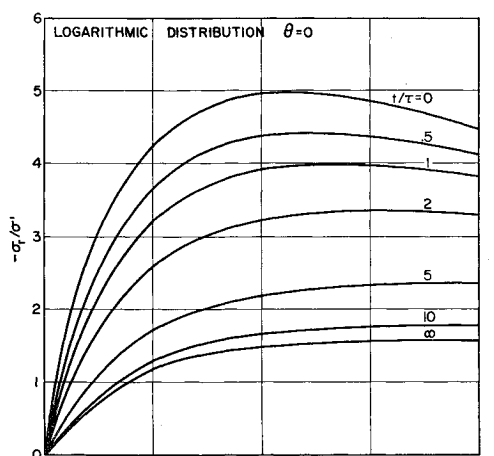

a)

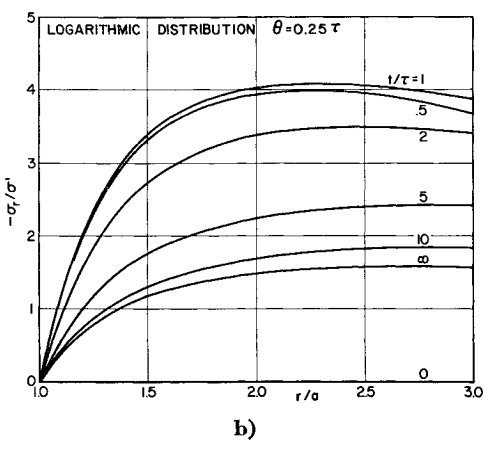

b)

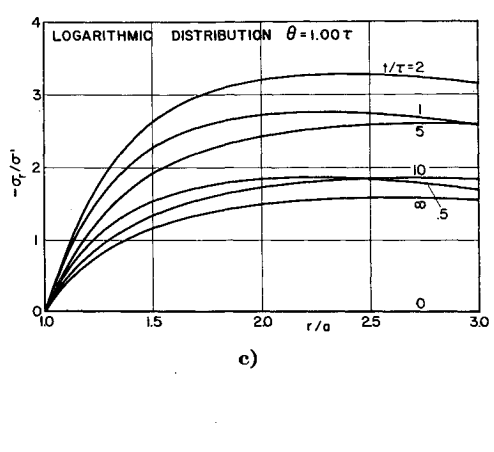

c)

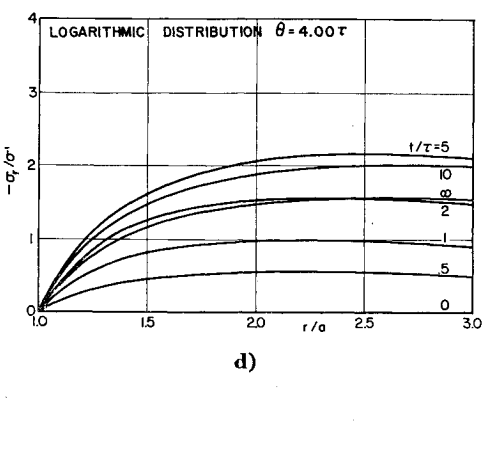

d)

Fig. 6 The radial stress as a function of (r/a).

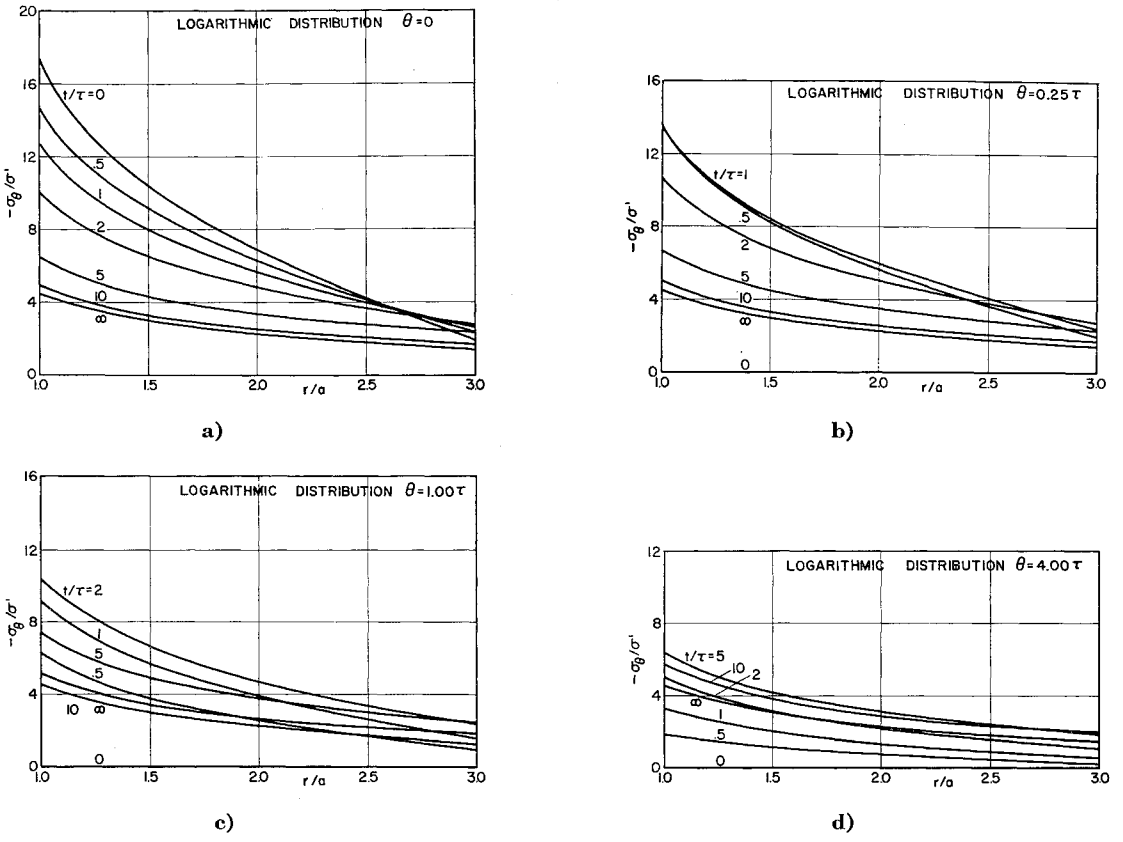

Fig. 7 The circumferential stress as a function of (r/a).

vals (t/τ) (0, 0.5, 1.0, 2.0, 5.0, 10.0), and also for the different loading rates, Figs. 5–7.

Conclusion

Since discussion of the closed-form solution equations (15) is not possible, the results of the numerical example will be discussed. The results exhibited in Fig. 4 show a marked reduction in the maximum values of the principal stresses with diminishing loading rates. The radial displacement is not affected, to any significant extent, by the loading rate. The maximum values of the principal stresses are achieved at different t/τ ratios for different rates of loading. For instantaneous loading ($\theta = 0$), the maximum principal stresses occur at once, but as the rate of loading decreases, a hump forms in the stress curves and moves in the direction of increasing t/τ, getting smaller for slow rates of loading. Even though the maximum values of the principal stresses depend on the rate of loading, the final values (at $t/\tau = \infty$) are not affected.

In Fig. 5 the values of radial displacement (u_r/u^1) are plotted as a function of space (r/a), for seven time periods (t/τ). The radial displacement always assumes its maximum value at the inner surface $(r/a = 1.0)$. It changes sign about $r/a = 2.0$ and has a minimum at about $r/a = 2.5$ before reaching zero at the outer surface. The rate of loading also affects this minimum. Although the final value (at $t/\tau = \infty$) of the radial displacement is not affected, lower values occur at intermediate times for slow rates of loading.

Figure 6 shows the dependence of the radial stress (σ_r/σ^1) on the loading rate. This maximum, which occurs at about $r/a = 2.5$, not only decreases for slower loading rates, but also occurs at different times (e.g., at $t/\tau = 0$ for $\theta = 0$, $t/\tau = 0.8$ for $\theta = 0.25\tau$, $t/\tau = 1.6$ for $\theta = 1.00\tau$, and $t/\tau = 5.5$ for $\theta = 4.00\tau$, as determined graphically from Fig. 4). The maximum radial stress is observed at about $r/a = 2.5$; however, at different times the point of maximum stress shifts to different positions. The maximum value of the final stress always occurs at the outer surface $(r/a = 3.0)$.

The forementioned observations also hold for the circumferential stresses (σ_θ/σ^1), Fig. 7, except that their maxima always occur at the inner surface $(r/a = 1.0)$.

This paper presents a possible solution to the nonuniform shrinkage problem of a medium with homogeneous time-dependent properties, where the shrinkage distribution is exponential in time but arbitrary in space. The problem of uniform shrinkage for a homogeneous medium has been presented by Freudenthal and Shinozuka,[4] where the shrinkage is assumed to be spontaneously caused by chemical reactions, therefore keeping the material properties homogeneous through the cylinder. This is an approximation if the shrinkage is caused by a temperature distribution. The present paper attempts to refine the forementioned approximation by taking into account the effect of temperature distribution on stresses and displacements while neglecting its effect on the material properties for the sake of expediency.

References

[1] Boley, B. A. and Weiner, J. H., *Theory of Thermal Stresses* (John Wiley and Sons, New York, 1960), Chap. VIII, p. 257.

[2] Churchill, R. V., *Modern Operational Mathematics in Engineering* (McGraw-Hill Book Co. Inc., New York, 1944), Chap. I, p. 2, Chap. IV, p. 157.

[3] Lee, E. H., "Stress analysis in viscoelastic bodies," Quart. Appl. Math. **13**, 183–190 (1955).

[4] Freudenthal, A. M. and Shinozuka, M., "Shrinkage stresses in a viscoelastic cylinder bonded to a rigid case," AIAA J. **1**, 107–115 (1963).